quaternary

MDPI

Article

Geoarchaeological Analyses of a Late-Copper-Age Kurgan on the Great Hungarian Plain

Péter Cseh [1,2,*], Dávid Molnár [1,2], László Makó [1,2] and Pál Sümegi [1,2]

[1] Department of Geology and Paleontology, University of Szeged, H-6722 Szeged, Hungary; molnard@geo.u-szeged.hu (D.M.); makol@geo.u-szeged.hu (L.M.); sumegi@geo.u-szeged.hu (P.S.)
[2] Long Environmental Changes Research Team, Interdisciplinary Excellence Centre, Institute of Geography and Earth Sciences, University of Szeged, H-6722 Szeged, Hungary
* Correspondence: cspeter@geo.u-szeged.hu

Abstract: Kurgans are the custodians of outstanding archaeological, natural and environmental-historical value in the lowland landscape of Eastern Europe, which has been continuously transformed over millennia by agricultural activity. Their protection and study are, therefore, essential. By comparative soil and sedimentological analysis of the soil levels buried during the kurgans' construction, the levels of buried soil, and the recent surface soil, we can gain information on the environmental changes of the second half of the Holocene; we can also gain information about how the activity of humans, even in the case of prehistoric cultures, can cause changes in the soil and environment on a local scale, beyond the regional scale. The aim of our research was to conduct a geoarchaeological examination of the Császárné Mound, which is one of the kurgans in the Hungarian Great Plain. For this purpose, sedimentological analyses (grain size distribution, magnetic susceptibility measurements), a pollen analysis, and a malacological analysis were carried out on the samples from the Császárné Mound. The complex geoarchaeological investigation of the mound allowed us to distinguish three different construction layers in the kurgan's soil material. Besides the archaeological results, we were able to reconstruct steppe-like environmental conditions before and during construction in the local surroundings of the kurgan.

Keywords: kurgan; Holocene; geoarchaeology; radiocarbon; pit grave; environmental history; Yamnaya; magnetic susceptibility; malacology; sedimentology

Citation: Cseh, P.; Molnár, D.; Makó, L.; Sümegi, P. Geoarchaeological Analyses of a Late-Copper-Age Kurgan on the Great Hungarian Plain. *Quaternary* **2022**, *5*, 20. https://doi.org/10.3390/quat5020020

Academic Editor: Ioannis Liritzis

Received: 1 November 2021
Accepted: 18 February 2022
Published: 3 April 2022

1. Introduction

With the emergence of archaeological cultures, in addition to natural sedimentary basins, the study of archaeological objects has been given priority in the reconstruction of the former Holocene environment. These objects can be defined as former settlement sites (tells, hillforts), shell mounds, or burial mounds—or so-called kurgans—in the Eastern-European steppes [1]. Besides kurgans of the Eastern-European–Western-Asian region and several types of mounds, tells and other archaeological objects, cultural layers are studied for geoarchaeological investigations into the Late Neolithic to the Bronze Age (for instance, in Mediterranean regions such as Anatolia [2], Palestine [3], and the Greek Islands [4,5]). These investigations can be connected to the study and dating of landscape evolution [6,7], and ultimately, they may also include changes in the connection between humans and their environment during the Holocene [8].

Kurgans are characteristic features of the lowland landscape, dating from the Late Copper Age–Early Bronze Age (3300–2500 BC). Most from that age are associated with the Yamnaya culture (the people of the pit-grave kurgan), which was present throughout the entire steppe zone of Eastern Europe and Western Asia [9] (Figure 1). This culture had a great influence on the cultures that followed (linguistic and cultural elements) [10]. The area of Hungary was the westernmost extension of the Yamnaya, a culture of stockbreeding

nomadic people who built these large mounds for funeral purposes. Their mounds can mostly be found on elevated areas along the banks of defunct rivers [11,12]. Besides the Yamnaya kurgans, many other nomadic cultures—such as the Scythians (900–100 BC), Sarmatians (600 BC–400 AD), Thracians (800 BC–100 AD), Hungarians (700 BC–Medieval) and Cumans (1300 BC–Medieval)—populating the Eurasian steppe and Carpathian Basin also built burial mounds for their noble people [13–15]. Moreover, in the case of cenotaphs (which were characteristic of Proto-Bactrian societies), tombs did not always contain the body for whom the monument was built [16]. Thus, the correct dating of these monuments is quite important in order to distinguish them from each other.

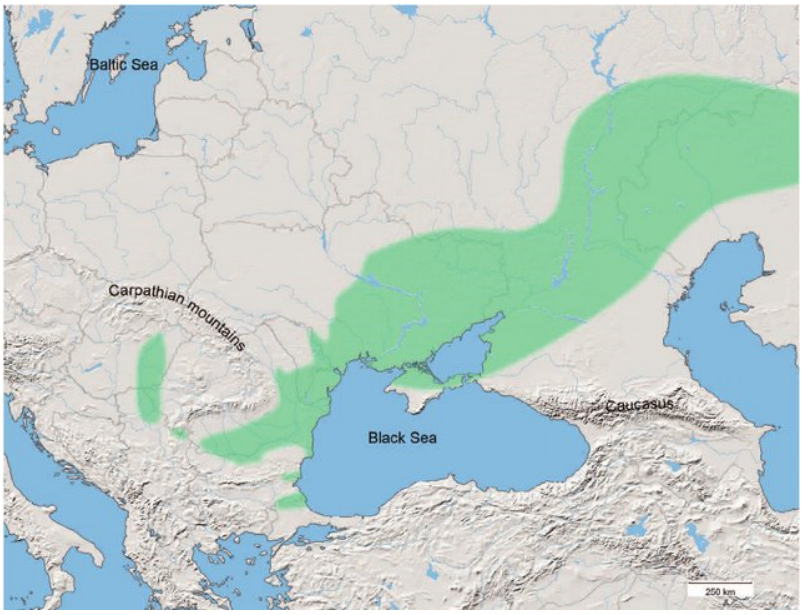

Figure 1. Geographical range of the Yamnaya Culture [17].

These kurgans were built as burial mounds and mostly consisted of several different construction layers, in which different soil and sediment strata can be studied [18]. They were built on the natural-ground surface, where the first burial site was established and the surrounding soil was used as building material [19–21]. Most of the time, loose soil material was used; however, there is proof of the use of complete soil blocks for construction [22]. In this way, the soils of the mounds were reworked. Thus, these can be considered disturbed anthropogenic soils with the characteristics of the original soil material, while the buried-former-soil horizon remains undisturbed. The changes in this reworked material can be detected, and can be compared with the undisturbed buried-soil profile.

The study of burial mounds in Hungary began in the 19th century, initially for archaeological, botanical and cadastral purposes [23]. From the 20th century onwards, geological and pedological methods began to be used to describe the stratigraphy of the mounds. Today, mound research no longer has only an archaeological role. The study of the soil; the paleontological, geochemical and sedimentary properties of the sediment; and the soil layers buried beneath the mounds make possible the reconstruction of the dynamic changes in the former environmental elements over time. As the various methods are refined, mounds have made paleoenvironmental research of the second half of the Holocene possible. The reason for this is that soils constantly develop due to climatic, landscape and ecological factors; in time, the soils' nature may be considered a result of these factors. However, because of their continuous evolution, it is difficult or impossible to reconstruct the former environment by studying recent soil. Kurgans provide places where the former soil has been buried by human mound-building activity, and they can preserve the factors that characterized the former environment via the buried soils [24].

Kurgans of the steppe environment were mostly made of soils developed from loessy material. They were created by using Chernozem soils [25]. The results of geoarchaeological surveys in recent years have paved way for paleoenvironmental reconstructions, which has allowed researchers to determine the intensity and direction of pedogenetic and diagenetic processes of soil formations in the last 5000 years [26–28].

For these reasons, buried soil and soil material of kurgans, beyond the descriptive pedological purposes, can be studied for the reconstruction of the former environment by pollen, or even pytholit examinations [1,29,30], thus, the former microenvironment of the surrounding of the mound can be reconstructed. Furthermore, the former fauna can be investigated by the examination of snail-shell remains in the sediment for a more accurate reconstruction of the kurgans' environment [31]. Thus, kurgans provide paleoenvironmental data about the Holocene and the environment of the former cultures, in addition to their archaeological relevance.

The Császárné Mound has never been subject to geoarchaeological investigations before. According to the National Museum Archaeological Database [32], investigations on the kurgan were carried out in recent decades (in 1983 and 2005). Based on the field survey of 1983, the mound was described by archaeologist Béla Kürt as a monument of the Yamnaya culture. This description also appears in later archive documentations [32], although a scientific study of the mound, and thus a more precise delineation of its origin and the separation of the actual construction layers, has never been proven. Therefore, the aim of this research is to clarify this issue.

Accordingly, this paper has two aims. Firstly, to distinguish the different construction layers of the kurgan by studying the soil and sediment material by sedimentological methods including loss on ignition, grain size analysis and magnetic susceptibility measurements. The second aim is to study the buried soil material below the kurgan to reconstruct the former environment of the kurgan's surroundings. For this aim, sedimentological, malacological, pollen analytical methods were used.

2. Study Area

The Császárné Mound (46°33′32.76″ N, 20°2′44.64″ E) is located in the central region of the Carpathian Basin (Figure 2), in the area of the Danube–Tisza interfluve region within the Great Hungarian Plain. The kurgan's area is part of the Kiskunság National Park, with an elevation of 91 m, the mound extends 6 m above the average 85 m of the surrounding plain.

A significant amount of alluvial Quaternary sandy sediments was deposited in the area as the former alluvium of the Danube River flowed through the area at the end of the Pleistocene. These sediments were transported and sorted into sand dunes by eolian activity at the end of the Pleistocene [24]. In addition, part of the Danube–Tisza area is also covered by loess, as a result of dust fall in the late Pleistocene. In the areas close to the Tisza, the occurrence of river-related floodplain sediments also became significant during the Holocene [33].

The soil conditions in the area are suited to the geological and climatic conditions. In the alluvium of the Tisza, significant meadow and alluvial soils have developed. The sandy areas are characterized by the presence of sandy soils and humic sandy soils, while the loessy–sandy bedrock areas are characterized by sandy soils of the Chernozem type. In less elevated areas, the groundwater levels are higher, thus meadow Chernozems also appear [34].

In terms of plant cover, the Carpathian Basin has been characterized by a mosaic environment since the Pleistocene. The most significant change at the beginning of the Holocene was the occurrence of a warmer and wetter climate phase which characterized the area of the central Carpathian Basin, and caused a vegetational shift from the cold-loving taiga, following which tundra elements completely disappeared and the forest-steppe vegetation with grasses and deciduous forests emerged [35]. Thus, today, among the vegetation belts of Hungary, the lowland region is naturally part of the forest-steppe belt, with steppe meadows, steppe scrub and a mosaic of oak forests with a looser structure [35].

Hungary, including the Danube–Tisza Interfluve region (Figure 2A), is located in the temperate climate zone. Three major climatic influences prevail in the Carpathian Basin, namely the western oceanic, the southern Mediterranean and the north-eastern dry continental influences. Based on the Holdridge classification system, which is based on the potential evaporation rate, the annual mean precipitation and mean annual temperature, the area is classified as cold temperate grassland [36]. According to the Péczely classification, it is placed in the warm and dry category [37]. The average temperature in the eastern part of the southern Great Plain is around 10.5 °C, the warmest month is July, with an average temperature of 21.8 °C and the coldest month is January, with an average temperature of 1 °C. The number of winter days is lowest in the basin compared to the rest of the year, while summer days are among the highest. The average annual rainfall is very low, between 500 and 550 mm per year, of which 300–350 mm falls during the growing season, making it one of the driest regions in the country. The average relative humidity is around 60% in July, which favors strong evaporation [37].

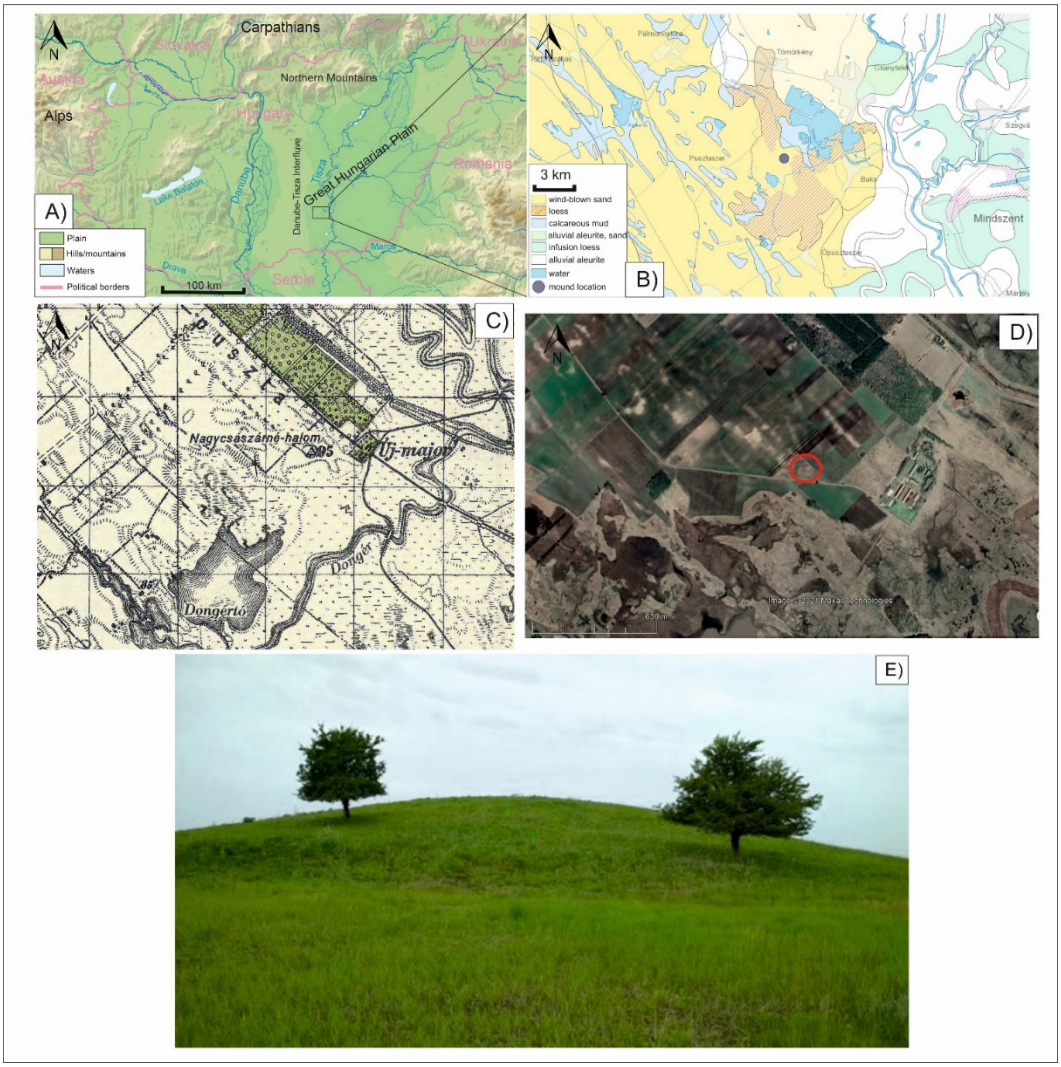

Figure 2. (**A**) Location of the Császárné Mound in Hungary [38], (**B**) Surface geological map of the vicinity of the study area [39] (**C**) The mound on the topographic map of Hungary in the period of World War II., [40] (**D**) Satellite image of the mound with its surroundings [41], (**E**), Császárné Mound (from the South) [Authors].

3. Materials and Methods

3.1. Sampling and Macroscopic Analysis

Sampling was carried out with a motorized spiral drill with a diameter of 10 cm in order to gain a sufficient amount of sample material for the different test methods. To prevent contamination caused by the open auger, the outer parts of the samples were removed and were not included in the further analysis of the sediments. Five boreholes were deepened into the mound, of which the central one, in the central part of the mound, was sampled every 10 cm with monotonous sampling [42]. The central drilling was selected for further analysis because it includes the full thickness of the mound and may have been less affected by agricultural disturbances. Thus, a total of 49 samples were collected for further analysis from the section of 490 cm. In addition to the thick-spiral drilling for the sampling in the central area of the mound, a geological cross-section was established along a transect approximately between 310° N and 130° S-SE, with four additional mapping geoarchaeological drillings. The mapping drillings, with a thickness of only 3 cm, were specifically designed for mapping purposes and were drilled to distinguish the different construction levels of the mound (Figure 3).

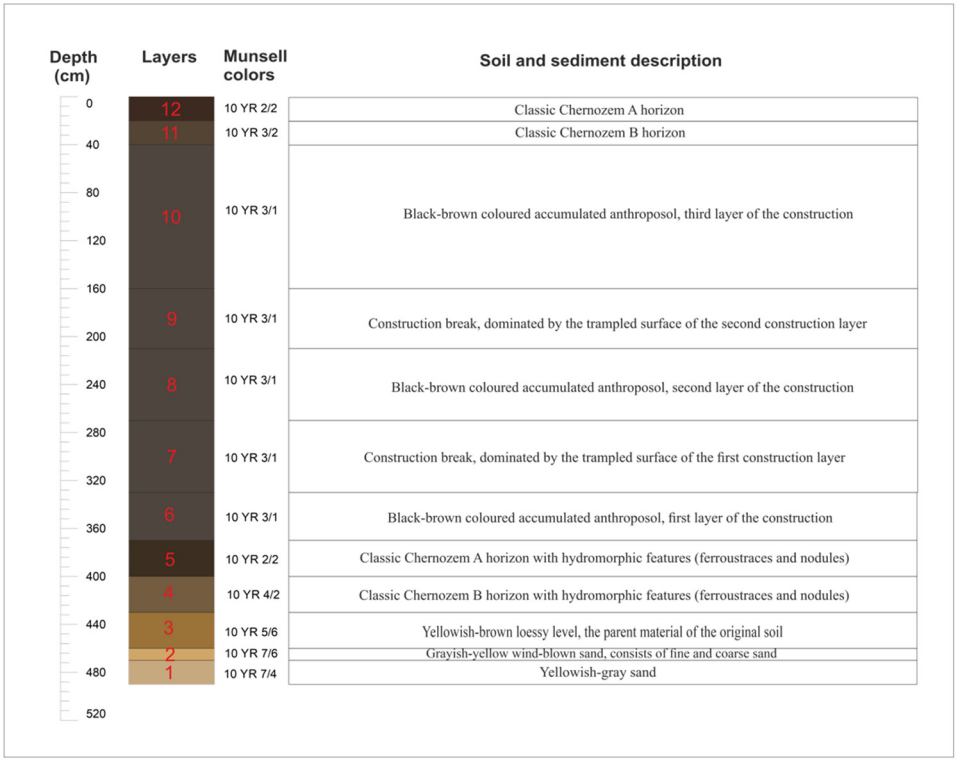

Figure 3. The different strata of the drilling log of the mound with short macroscopic descriptions. Red numbers: (1). Yellowish-gray sandy layer, (2). Grayish-yellow sandy layer, (3). Yellowish-brown loessy layer, (4). Buried soil layer B horizon, (5). Buried soil layer A horizon, (6). First construction layer of the mound (7), The compact-structured, trampled section of the first construction layer, (8). Second construction layer of the mound (9). The compact-structured, trampled section of the second construction layer, (10). First construction layer of the mound, (11). Recent surface soil B horizon, (12). Recent surface soil A horizon. The different layers are colored according to the RGB color of the described Munsell color categories.

Coordinates of the geoarchaeological mapping drillings are as follows:

- I.: N 46.55915708°, E 20.04552992°, 88.59 m altitude (depth: 3.7 m);
- II.: N 46.55911706°, E 20.04564056°, 90.52 m altitude (depth: 4.0 m);
- III.: 46.55906689°, E 20.04584153°, 91.31 m altitude (Drilling section, depth: 4.9 m);
- IV.: N 46.55901792°, E 20.04602844°, 89 m altitude (depth: 4.1 m);

- VI.: N 46.55906438°, E 20.04612621°, 87.46 m altitude (depth: 4.0 m).

General stratigraphy of the sediment and soil layers was identified at the site, and the wet color of the samples was defined using the Munsell Color Chart [43]. These provided a reliable basis for the further characterization of the different sediment and soil layers. The soil layers were identified based on the Hungarian Soil Classification System [34], which can be used for the exact identification of the different subtypes of Chernozem soils. This system can be correlated with the WRB's classification [44,45]. Based on these two systems, Classic Chernozem soil can be considered as Chernozem, while meadow (hydromorphic) Chernozem as Gleysols. Thus, from a soil genetic point of view, meadow Chernozem is a more accurate denomination for a Chernozem-like soil that is affected by the fluctuating groundwater.

3.2. Grain Size Analysis

The grain-size composition was determined based on the principles of Bokhorst [46]. Before the measurements, samples were pre-treated with hydrogen peroxide (30% H_2O_2) and hydrochloric acid (10% HCl) to remove organic material and carbonate from the samples. Then, 30 mL of the sodium hexametaphosphate ($Na_2P_6O_{18}$) solution was added to 0.7 g of the sample to separate the individual granules and, for the same reason, samples were treated in an ultrasonic cleaner. However, this process destroyed the carbonate content of the samples; it should be noted that the carbonate content of this sediment was not in granular form due to secondary dissolution processes. The prepared suspensions were filtered through a 0.5 mm sieve, but the amount of remaining sediment was practically negligible. The grain-size composition measurements were carried out at the Department of Geology and Paleontology, the University of Szeged with an Easysizer 20 laser sedigraph. To achieve this, a 2 MW energy and a 0.6328 µm wavelength He-Ne laser was used [47]. The laser sedigraph measured 42 particle size ranges between 0.0001 and 0.5 mm using 54 built-in detectors. The results were arranged into particle size ranges based on the Wentworth scale [48] and plotted on line diagrams.

3.3. Magnetic Susceptibility Analysis

Magnetic susceptibility measures the magnetizable-element content of sediments. The measurements were carried out on bulk samples that were homogenized in a glass mortar before the measurements. A Bartington MS2 Magnetic Susceptibility Meter at a frequency of 2.7 MHz [49] was used for the measurements. A minimum amount of material for the measurements was available. Three measurements were performed on each sample and the obtained values were averaged. In this paper, the noted magnetic susceptibility values are considered in the value $\times 10^{-8}$ m^3 kg^{-1} SI scale.

3.4. Loss-On Ignition

To determine the organic matter and carbonate content, Dean's loss on ignition method was used [50,51]. This method is commonly used for the determination of carbonate and the organic matter content of carbonaceous sediments. Firstly, after air-drying for 24 h at 65 °C, the 49 samples were homogenized in a porcelain mortar. The weight of the crucibles was measured to the nearest 0.0001 g (m_c), and approximately 3 g of the sample was added. Then, the crucibles were heated at 105 °C (24 h) and measured (m_{105}). After heating at 550 °C (2.5 h), the crucibles were measured (m_{550}) again and the organic matter content was calculated, and after heating at 900 °C (2.5 h), the crucibles were measured again on the same samples and the carbonate content was calculated based on the following equations:

$$\text{Organic matter content (\%)} = 100 - ((m_{550} - m_c)/(m_{105} - m_c)) \times 100$$

$$\text{Carbonate content (\%)} = 100 - ((m_{900} - m_c)/(m_{550} - m_c)) \times 100$$

The calculated organic matter and carbonate contents can be considered as the TOC (Total Organic Carbon) and TIC (Total Inorganic Carbon) contents of the samples. After

obtaining these measurements, the percentage of organic matter, carbonate content and inorganic matter (or mineral content) of the sediment samples were calculated.

3.5. Radiocarbon Dating

Furthermore, AMS 14C radiocarbon dating was carried out in the Nuclear Research Center of the Hungarian Academy of Sciences in Debrecen (Hungary). A total of seven samples were measured for radiocarbon. A total of six samples originated from soil organic matter. One sample's radiocarbon age was measured by using an *Unio* mollusk shell fragment. The preparation of the samples and the measurements were based on the methods of Hertelendi et al. [52] and Molnár et al. [53]. Bulk samples were used for radiocarbon measurements of the organic C content of the soil samples. The shell was selected because previous studies [54,55] have shown that correct ageing could be determined using such shells. Periostracum was no longer present on the shell. The umbo part of the left valve was measured. The outer layer of the shell (ostracum) was cleaned mechanically and the inner (hypostracum) was cleaned chemically [56] to exclude any carbonate that may have been subsequently precipitated on the shell surface. The sample for the radiocarbon measurement was taken from the interior nacre layer because the prismatic outer layer was damaged by mechanical cleaning. In relation to the measurements of the isotopic composition of ostracum and hypostracum layers of recent *Unio crassus* individuals [57], the difference was minimal (between 0 and −0.2‰ for $\delta^{18}O$). Thus, the hypostracum layer is suitable for chronological studies and a correct age can be obtained by its analysis [55]. Due to the errors of the measurement, the lifespan of the studied shells does not influence the chronological age.

The conventional radiocarbon ages were converted to the calendar and BP ages using IntCal 20 calibration curves [58], and are presented here with a 2-sigma confidence level (>95% for each sample). The potential problem with the radiocarbon measurements is the reservoir effect, because of which, the ages calculated by calibration do not provide the exact age, but the maximum age of the samples. The real age of the samples may be less than the calibrated ages [59]. From the soil samples 3-3 measured from L-fraction (extracted on 400 °C) and H-fraction (extracted on 800 °C from the same sample), respectively.

3.6. Malacological Analysis

For the malacological analysis of the Császárné Mound, samples were taken at every 10 cm and washed through a 0.8 mm sieve to remove sediment. The snail shells were sorted and identified according to the malacological protocol developed by Krolopp [60]. Thus, a total of 49 samples were considered in the analysis from the borehole section of 490 cm. The samples had approximately a 0.4 kg wet weight, compared to 2.7 kg sediment as suggested by Krolopp. Although the numbers of Mollusca fauna were quite low, they can be used as environmental indicator elements. This makes the fauna an excellent tool for reconstructing the environment before and during the construction of the kurgan. Due to the lack of the possibility for statistical evaluation, the species were tabulated according to whether or not they were found in the different strata.

3.7. Pollen Analysis

The standard *Lycopodium* spore tablet method was used for the pollen analysis [61]. The use of the conventional 1 cm^3 of material did not yield valuable results, so 200 g of wet sediment was used for the analysis. Known concentrations of *Lycopodium* spore tablets were added to each sample for the determination of pollen concentrations. Pollens were identified and counted using a light microscope at 400–1000× magnification. For the identification, the database of the Department of Geology and Paleontology, University of Szeged and pollen atlases were used [62,63]. The minimum pollen count per sample was set at 300 pollen grains following the work of Maher, Sümegi et al. and Magyari et al. [61,64,65], whereby a pollen sterile sample is defined as one in which the number of pollen and spores

per sample is below 80 [65]. The pollen results are presented in Tables 1 and 2. A total of 300 pollen grains were recovered from all samples.

Table 1. Pollen composition and proportion of arboreal pollen (AP) material extracted from the samples of Császárné Mound.

Depth (cm)	*Pinus sylvestris*	*Fagus*	*Carpinus*	*Quercus*	*Salix*	*Tilia*	*Ulmus*	AP Total
	%	%	%	%	%	%	%	%
360–370	9.01	0.85	1.97	3.94	4.79	0.28	1.41	**22.25**
370–380	9.51	1.15	2.31	4.61	5.48	0.29	2.02	**25.36**

Table 2. Pollen composition and proportion of non-arboreal pollen (NAP) material extracted from the samples of Császárné Mound.

Depth (cm)	*Achillea* type	*Artemisia*	*Cerealia*	*Chenopodiaceae*	*Compositaea*	*Plantago lanceolata*	*Poaceae*	*Polygonum aviculare*	*Taraxacum*	*Verbascum*	NAP
	%	%	%	%	%	%	%	%	%	%	%
360–370	0.85	2.82	0.85	4.23	1.41	1.69	64.51	0.28	0.85	0.28	**77.75**
370–380	0.58	1.73	0.58	3.17	1.73	1.73	63.69	0.58	0.29	0.58	**74.64**

4. Results

4.1. Results of Stratigraphic Mapping Drillings

The five spiral drillings made the distinction between different layers in the kurgan possible. Natural sediment layers and the different soil layers were identified.

Sandy and silty sediments were found at the bottom of the drillings under the construction layers of the kurgan which is considered as the natural bedrock of the kurgans surroundings. These layers can be observed much closer to the surface in the outer parts of the kurgan.

Based on a macroscopic analysis of the drill sequence, the kurgan was built by several construction phases. These layers can be distinguished from each other by their soil structure despite their colour being similar (Figure 3) The first construction layer was built with a thickness of 1.2–1.5 m above the former soil surface. Towards the edges of the mound, this layer was tapered by later human impact (plowing activity).

The top of the next layer had a more compact horizon than the soil material below. The second layer was conically spread over the surface of the first layer. The central part of the layer was 100 cm thick and the edges 40 cm, but its development was highly variable on the edges, which held the remains of planting pits. Marks of digging and disturbance were highly visible here. Both phenomena can be distinguished by a less compact structure and darker color which were noticed on the field. On the other hand, the third layer on the top of the kurgan was 120–130 cm thick in the central part of the mound, but only 40–80 cm thick at the edges based on our drillings. It is also distinguished by the compacted surface horizon of the second layer below (Figure 3).

At the edges of the third layer, subsequent human impact has resulted in a collar-like terrace level probably used for cultivation. A significant erosion trench is observable at the edge of the terraced surface (steeper slopes in Figure 4). It can be assumed that the third construction layer has the loosest structure in the kurgan, and on its edges, it can be seen that the surface of the more compacted second layer was used to form a walking level for agricultural work, which caused its transformation into a terraced surface via trampling. On the mapping drillings, the trampled surfaces cannot be observed. In the sections of

these boreholes, the steeper parts of the kurgan are characterized by a lower thickness of the kurgan's soil material than the central parts (Figure 5).

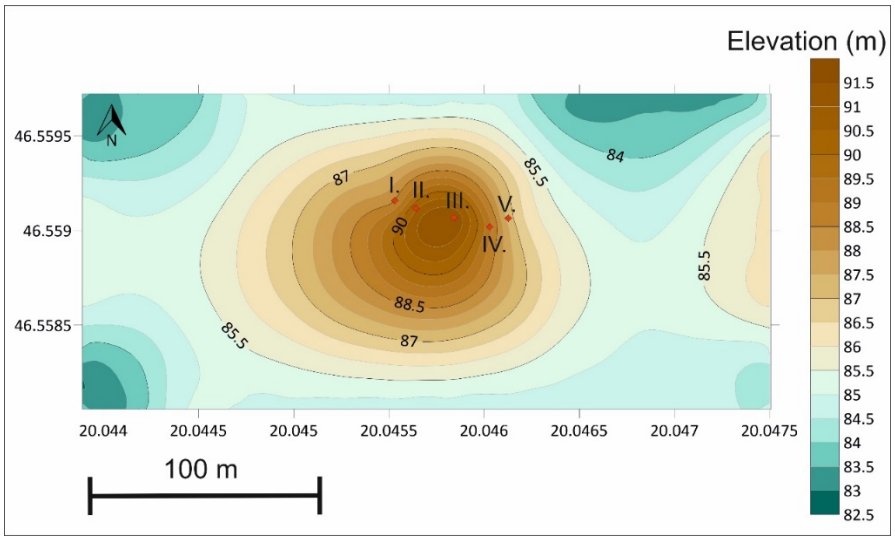

Figure 4. The geomorphology of the mound and its surroundings. Red squares with numbers are the mapping drillings and the central drilling (III.) from where the samples for the measurements were yielded from.

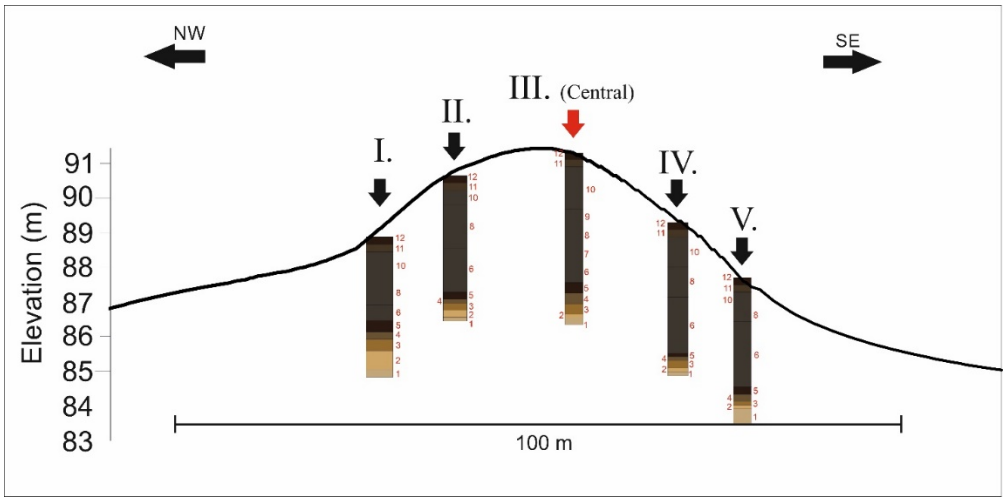

Figure 5. NW-SE transect of the mound and its different sediment and soil layers. Roman numbers: boreholes. Red numbers: (1). Yellowish-gray sandy layer, (2). Grayish-yellow sandy layer, (3). Yellowish-brown loessy layer, (4). Buried soil layer B horizon, (5). Buried soil layer A horizon, (6). First construction layer of the mound (7), The compact-structured, trampled section of the first construction layer, (8). Second construction layer of the mound (9). The compact-structured, trampled section of the second construction layer, (10). First construction layer of the mound, (11). Recent surface soil B horizon, (12). Recent surface soil A horizon. The different layers are colored according to the RGB color of the described Munsell color categories.

4.2. Results of the Sedimentological and Pedological Studies

In the lowest part of the drilling section of the Császárné Mound between 470–490 cm, yellowish-grey (10 YR 7/4) sediment can be found. It can be characterized by a significant sand proportion (more than 15%). Based on its low organic-matter content and macroscopic observations, no soil formation can be observed. It has a high carbonate content of more than 10%, which is significantly high in the whole layer. Above this, between 460–470 cm,

a greyish-yellow carbonaceous sandy silt can be found. Its organic matter is still low, the carbonate content is 13% and the proportion of the sand fractions is more than 30%. The clay content of both sandy layers (15%) is not significant compared to the rest of the mound's sediment (Figure 6).

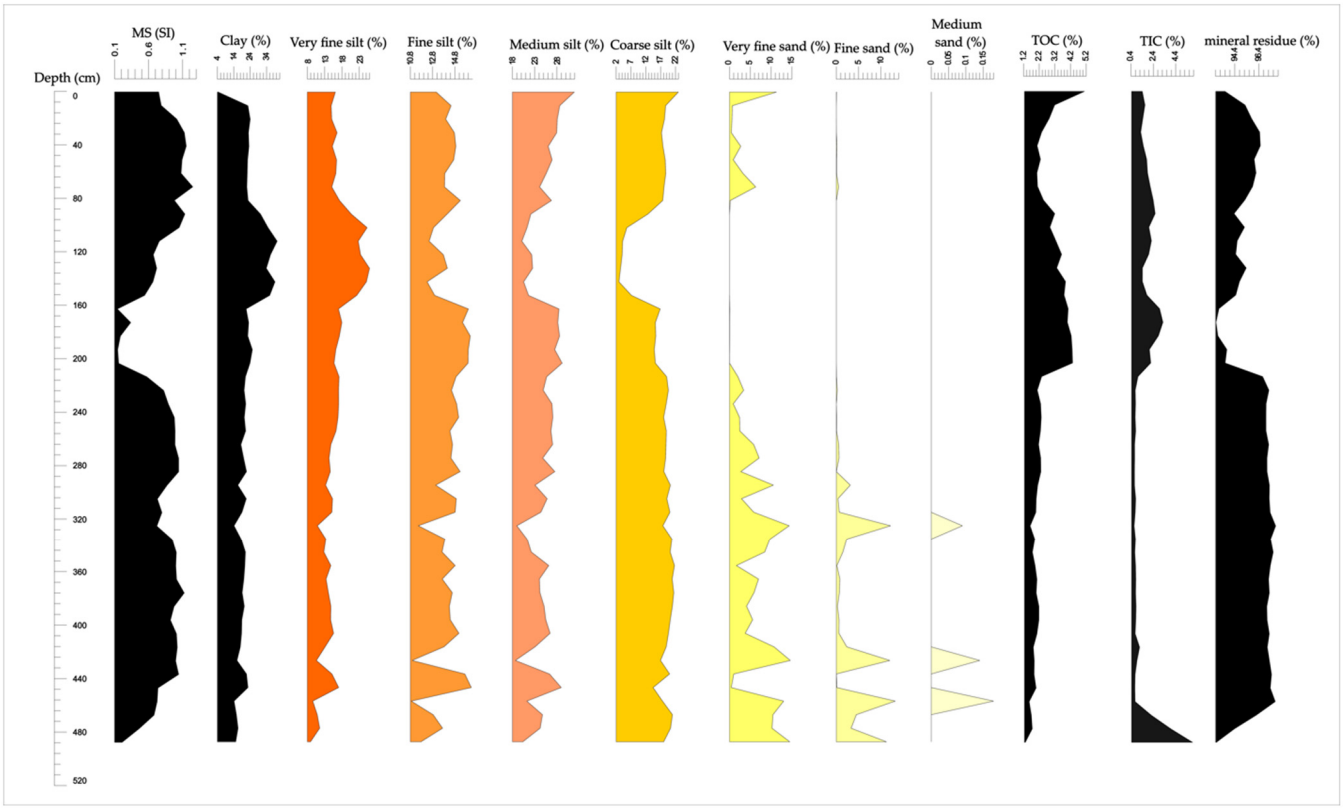

Figure 6. Results of the magnetic susceptibility measurements, grain size distribution and LOI measurements on the samples of 490 cm borehole of Császárné Mound.

A loessy layer was deposited on the top of the sand (between 430–460 cm) (Figure 6). It can be characterized as having a yellowish-brown color (10 YR 5/6), low sand content, low carbonate and increasing organic-matter content. These facts indicate the development of soil formation processes at this layer.

These processes indicate the formation of the original former-soil (now subsoil) layer. The A horizon (between 370–400 cm) (Figure 6) of the soil layer formed on the loessy sediment shows classic Chernozem soil features (color: 10 YR 2/2), but hydromorphic properties can also be observed, such as iron concretions and spots. In its B horizon (color: 10 YR 2/2) (400–430 cm), the leaching processes characteristic of Chernozem can be observed as having a more significant carbonate content. Meanwhile, the macroscopic hydromorphic properties are also observable in this horizon. The most important feature of this soil horizon is that it has a higher organic-matter content (than the loessy and sandy parts below) and that, in addition to the classical Chernozem, hydromorphic meadow soil properties also can be observed. The crumbly structure of Chernozem and the polyhedral meadow soil structure also appear concurrently. At these levels, the clay content reaches 20%, but the silt fractions dominate the sediment (Figure 6). Based on these properties, these two levels can be identified as an A and B horizon of a meadow Chernozem [34].

Three construction phases can be distinguished within the mound body, which is built on the former soil surface (now its subsoil layer) (Figure 3). The first construction layer, between 370–270 cm (Figure 3), is of a blackish-brown soil material (10 YR 3/1), a human-influenced disturbed anthroposol. The soil material between 270–330 cm may have

been a former soil surface, based on its compacted, trampled structure properties. Its grain composition and organic matter content are the same as the level of the subsoil (Figure 6).

The second construction layer (between 270–160 cm) (Figure 3) is of a blackish-brown (10YR 3/1) soil material and has a similar grain-size composition as the first layer. The most significant differences are in the organic-matter content and carbonate content. Based on the organic-matter content, on the top of the construction level, a new former surface was developed as a break in the mound construction. The organic matter content on the upper part of this level reaches 4%, and the carbonate content becomes detectable at significant (3.2% maximum) values for the first time in the mound's body (Figure 6).

Significant differences can be observed in the third construction layer (from 170 cm to the surface). The proportion of the clay fraction reaches its maximum of 40% and remains above 20% in the whole layer. The proportion of silt fractions is about 50–60%. Relatively high organic matter and carbonate content (3.8% and 3.8%, respectively) can be observed (Figure 6). Based on these data, this layer can no longer be characterized as meadow soil, but a classic Chernozem.

The blackish-brown (10 YR 3/1) soil layer formed on the surface of the kurgan. The grain composition is the same as in the layer below, the organic matter content reaches its maximum of 5% then gradually decreases towards the B level. In contrast, the carbonate content increases towards the B horizon (Figure 6).

4.3. Magnetic Susceptibility (MS) Results

The MS values of the bottom part of the drill sequence (between 490–430 cm), in the sand and loessy layers, are minimal (0.68×10^{-8} m^3 kg^{-1} maximum), which indicates the absence of soil formation. Between 370 and 430 cm, it starts to increase in the B and A horizon of the subsoil (Figure 6), which suggests soil formation by increased weathering and the increasing amount of iron-bearing minerals.

The first construction layer (270–370 cm) (Figure 6) can be characterized by high MS values (above 1) (Figure 6). These values were constant in the whole layer, with the exception of a decrease to around 0.72–0.79. This level may indicate a former construction break, where soil-formation processes became more intense.

The second construction level is the most characteristic level for MS. Between 160 and 270 cm, it is characterized by a change in MS values. In the lower part, the MS values approach 1 as in the case of construction level 1. In contrast, in the upper part they range from 0.14 to 0.19, which are the lowest values for the entire section. For this reason, an application break can be reconstructed with a former open soil surface, on which soil formation continued under different conditions than before, because of the elevated position. These processes can be observed in the change of the MS values.

In the third construction layer of the kurgan (from 160 cm to the surface), the MS values of the soil material increase again and reach 1. This is the same as the values of the first construction level of the kurgan. Based on this, the kurgan could be constructed from a similar soil material. MS values ranged from 0.75 to 1.16, and based on MS values, the process of recent soil formation may have affected the uppermost 40–50 cm. The low MS values correlate with the water-free, uplifted environment formed by the construction of the kurgan, since the elevated soil horizon cannot be affected by the fluctuation of groundwater which can cause the accumulation of the iron-bearing minerals that cause high MS values. Thus, a different (classical Chernozem) soil could be formed on the surface (Figure 3).

4.4. Results of Pollen Analysis

The proportion of the arboreal pollen in the subsoil and in the first construction layer was around 25% (Table 1). Based on Allen et al., Behre, Elenga et al., Magyari et al., Prentice et al., Prentice and Webb, and Tarasov et al. [66–73] studies on pollen composition, before the formation of the kurgan, even at the beginning of the Holocene, the area could have been a moderate steppe based on the AP: NAP ratio (Arboreal Pollen: Non-arboreal

Pollen). In addition to oak, beech and hornbeam pollens appeared in the material of the kurgan (Table 1).

The herbaceous vegetation was dominated by grasses (*Poaceae* = *Gramineae*) (Table 2), and a significant proportion of *Artemisia and Chenopodiaceae* in the soil level before the formation of the kurgan. In the soil material of the layers studied, the presence of a small proportion of weeds indicates animal husbandry and human disturbance. The presence and proportion of non-arboreal plants indicate a steppe-forest or steppe environment (*Polygonum aviculata, Compositae*). Human presence can be further proved by the presence of cereals (*Cerealia*).

4.5. Malacological Results

At the bottom, in the sandy sediments of the section between 460–490 cm, only aquatic species and *Succinea oblonga*, a typical species of wet meadows, were detected. In addition, a relatively high number of species, which tolerate variable water cover and occasional drying or ponding conditions (*Pisidium, Lymnaea truncatula, Anisus spirorbis*) (Table 3), were identified. Moreover, snail shells of *Planorbarius corneus, Planorbis planorbis* were also have found (Table 3), which indicates a more stable water cover. The presence of aquatic mollusk species in the quaternary deposits clearly indicates a strong water influence during the formation of the quaternary deposit sediments in the bottom of the section (460–490 cm). On the other hand, the presence of periodic water-preferring species in the bedrock suggests periodic water influence on the development of the soil. These malacological data also support the hydromorphic characteristics of the original Holocene soil that developed in the area.

Table 3. Mollusc fauna of the Császárné Mound in the different layers of sediments, soils and bedrock, distinguished by sedimentological and pedological analysis. 1: A horizon of the recent Chernozem soil covering the kurgan's surface, 2: B horizon of the recent chernozem covering the kurgan's surface, 3: Third construction level 4: Second construction level, 5: First construction level, 6: A horizon of the buried subsoil under the kurgan, 7: B horizon of the buried subsoil under the kurgan, 8: Loessy bedrock of the kurgans subsoil, 9/10 Sandy fluvial and aeolian sediments. "0" means that the species is absent from the layer. "+" means that the species can be found in the layer.

Species/Stratum	1	2	3	4	5	6	7	8	9	10
Lymnaea truncatula	0	0	0	0	0	0	0	0	0	+
Planorbis planorbis	0	0	0	0	0	0	0	0	0	+
Anisus spirobis	0	0	0	0	0	0	0	0	+	+
Pisidium	0	0	0	0	+	+	0	0	0	+
Succinea oblonga	0	0	0	0	+	+	0	0	0	+
Chondrula tridens	+	+	+	+	+	+	+	+	+	0
Helicopsis striata	0	0	0	+	0	+	+	+	+	0
Pupilla muscorum	0	0	0	+	0	+	+	+	0	+
Vallonia costata	+	+	+	+	+	+	+	+	+	+
Vallonia pulchella	+	+	+	+	+	+	+	+	+	+
Cepaea vindobonensis	+	+	+	+	+	0	+	+	+	0
Helix pomatia	0	0	+	+	+	+	+	+	0	0

In the buried soil layer, the combined presence of species typical of steppes (*Pupilla muscorum*) (Table 3), forest-steppes (*Vallonia costata, Cepaea vindobonensis, Helicopsis striata, Helix pomatia*) and wet meadows and waterfronts (*Succinea oblonga, Vallonia pulchella*) (Table 3), indicates a mosaic vegetation pattern with more significant vegetation cover in some places.

The same fauna can be detected in the first construction layer of the kurgan body, directly above the original Holocene soil layer (Table 3). This clearly indicates that the first layer was built using the natural soil material of meadow Chernozem. The second and third construction layers of kurgan were also relatively rich in snail shells. This indirectly supports the results of the higher carbonate-content values of the loss on ignition measurement.

Only shells of dry steppe elements were found in the section of the kurgan from 430 cm to the surface (Table 3). All the snail species recovered from the upper 370 cm of the kurgan are typical of dry steppes and forest-steppes (Table 3).

4.6. Chronological Results

A total of seven radiocarbon measurements were carried out on the samples of the Császárné Mound, which originate from three important horizons of the kurgan (Table 4). Three are from the horizon between 360–370 cm, which was the macroscopically observed first construction layer, two from 350–360 (also the first layer) and two from the third construction layer of the kurgan. From this data, six measurements were performed on soil organic carbon from bulk samples and one was obtained from an *Unio*-shell remain from the first layer (Table 4).

Table 4. Results of the radiocarbon measurements on the Császárné Mound.

Lab Code	Material	Depth (cm)	14C yr BP	±	Cal BP yr	±	Cal BC
DeA-21607	soil organic C	130–140	5589	32	6354	54	4459–4351
DeA-21606	soil organic C	130–140	5306	32	6094	100	4245–4045
DeA-21604	soil organic C	350–360	5552	46	5350	59	4460–4332
DeA-21605	soil organic C	350–360	6062	39	6898	106	5055–4843
DeA-21608	*Unio* shell	360–370	4506	33	5175	129	3355–3097
DeA-21602	soil organic C	360–370	5552	35	6345	54	4450–4342
DeA-21603	soil organic C	360–370	5913	33	6729	68	4848–4712

The non-calibrated data provided very similar dates from soil organic carbon from every depth (130–140 cm, 350–360 cm, 360–370 cm), of around 5.3–6 ka, and the calibrated years gives the ages of the soil samples as between 5350 ± 59 and 6898 ± 106 cal BP years. It can be stated that there is no significant difference between the dates of the first construction layer and the third construction layer. The age of the *Unio* shell from the first layer provides the youngest data of the seven measurements (5175 ± 129) even though it derives from the lowest construction layer.

5. Discussion

The sediment samples from the borehole section of the kurgan represent the former natural sedimentary environment before the construction of the kurgan. The area was mostly sandy in the first half of and before the Holocene. Based on literature, the former Danube alluvial sediments and an environment with sand dunes characterized the area, which was later covered by loessy sediment. These data fit well into the model of the Late Pleistocene and Holocene evolution of the Great Plain [33]. Soil formation may have begun for these sediments during the first half of the Holocene. At this time, the water regime of the area was already dominated by the proximity of the Tisza River, high water table and flooding, which is reflected in the hydromorphic properties of the developed soil [33].

The data from drilling on the kurgan was agreeable with this background. Based on the macroscopic study of the samples from the drillings, the Császárné Mound was built on a former riverbank, rising 1–1.5 m above the area, consisting mainly of sandy sediments and later covered by loess. In this former riverbank, meadow Chernozem soil formed. This hydromorphic soil was used to build the body of the constructed kurgan, which developed

into a classic Chernozem soil due to its elevated position and the lack of the groundwater effect. In the kurgan's soil, three basic levels could be distinguished (five if the compacted trampled surfaces of the first and second construction layers are distinguished) based on changes in grain composition, organic-matter content and MS.

Based on the grain-size composition of the kurgan's soil, the kurgan was built using the former soil horizon which is now buried. The peaks and trends of the organic matter content, measured by LOI, show the sections in which the accumulation of organic matter was higher, which suggests the presence of former soil surfaces. The lack of carbonate in the lower parts of the kurgan suggests that carbonate could have leached out and thus has not remained in its original position in this layer. In contrast, the upper layers contain more carbonate. This indicates differences between the two phases. The lower layers were more exposed to groundwater and thus the carbonate was more easily displaced, while the upper layers have a higher carbonate content, suggesting that the water balance of this soil was controlled by precipitation rather than groundwater.

Based on the MS, the kurgan was created with three construction phases in three different stages. The characteristic pattern of MS values parallels well with the evaluation of results from other mounds [1]. The significant decline in the magnetic-susceptibility signal, which characterizes the three construction layers of the mound, are consistent with the layers of the Lyukas Mound. In addition, the Ecse Mound and the Őr Mound show the same decline associated with the MS signal, due to the strong soil-erosion processes of the former open surfaces [1,18]. Using these methods together is essential. The analysis of the grain size distribution of samples alone provides a satisfactory answer for the separation of the sediment and soil levels, but not for the separation of the construction levels of the kurgan. Therefore, they should be used together. The bottom Quaternary sediments (up to 430 cm) (Figure 7) are well separated in both MS and organic matter and particle composition from the kurgan's soil. In the buried undisturbed soil layer (370–430 cm) (Figure 7), it can be observed that the increasing organic matter and clay content of soil formation is associated with an increasing MS signal. Relatively constant values of MS, grain composition and organic matter content were observed in the first construction layer (270–370 cm), so a macroscopic evaluation has to be included here so as to separate the first and second construction layers (Figure 7).

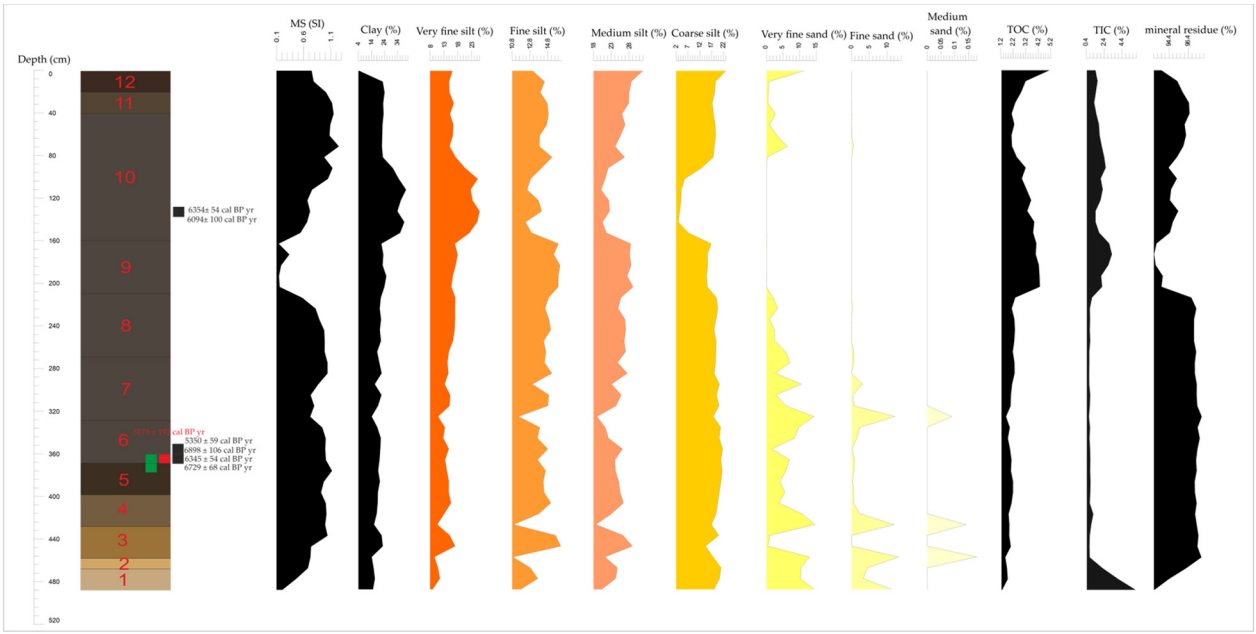

Figure 7. The strata of the central borehole of 490 cm of the Császárné Mound. Besides the results of magnetic susceptibility measurements, grain size distribution and LOI measurements on the samples of 490 cm borehole of Császárné Mound. Red numbers: (1). Yellowish-gray sandy layer,

(2). Grayish-yellow sandy layer, (3). Yellowish-brown loessy layer, (4). Buried soil layer B horizon, (5). Buried soil layer A horizon, (6). First construction layer of the mound (7), The compact-structured, trampled section of the first construction layer, (8). Second construction layer of the mound (9). The compact-structured, trampled section of the second construction layer, (10). First construction layer of the mound, (11). Recent surface soil B horizon, (12). Recent surface soil A horizon. The different layers are colored according to the RGB color of the described Munsell color categories. Black squares: cal BP yr age of soil OM. Red square: cal BP yr age of the *Unio* shell fragment. Green squares: The depth of the samples used for pollen analysis.

In contrast, in the uppermost part of the second construction layer (260–270 cm) and the lowermost part of the third construction layer (from 160 cm), the high clay and finer silt content are consistent with the high organic matter content in the lower part of the first construction layer and the uppermost part of the second construction layer, where, in turn, the expected high MS no longer appears, but a significant decrease occurs, which is in contrast to the clay content (Figure 7). These inconsistencies can be explained by the fact that in the first construction layer and in the buried soil, the effect of fluctuating groundwater was still more pronounced (presence of iron spots), in contrast to the second construction layer (especially its upper parts), where, despite the strong soil formation, the presence of iron minerals was less significant. This can be paralleled with the macroscopic observations of the transition of the hydromorphic soil to classical Chernozem. Similar results can also be observed for kurgans in similar environments on the Great Plain [18].

Based on the data, in the case of mounds that are investigated by simpler drilling methods without disturbing the mound body for reasons of nature conservation (e.g., exlege protection of the Hungarian Cumanian mounds) or cost-effectiveness, MS measurements with LOI and grain-size composition could provide a good basis for the separation of different archaeological deposition levels. Although the more pronounced presence of the construction layers can be well clarified by other non-destructive methods capable of providing useful results for the separation of the actual construction levels, the subsoil and the sediment, such as the loss on ignition that we have used, as well as the grain-size distribution of the different layers. In addition, a geochemical analysis of the sediments of the mound and the micromorphological analysis of undisturbed samples could also yield significant results, which can be a future aim of our investigations.

Whether a new burial chamber was formed in the second construction phase cannot be overlooked, as it was common in the case of burial mounds [11] but neither the basic pit grave nor the grave presumed to be in the kurgan were revealed, and bones were not recovered from the section. This in itself does not prove the absence of a central grave, but leads us to consider that graves in kurgans may be present in the outer parts, as is the case with the Sárrétudvar Őr Mound [74].

The radiocarbon analysis of individual samples raises some questions but also provides information. For the dating of the soil samples, soil organic-matter of bulk samples was used. The oldest soil sample was dated back to 6898 $\pm$ 106 cal BP yr, while the youngest soil was dated back to 5350 $\pm$ 59 cal BP yr (Table 4) (depth of the samples on Figure 7). Based on this, it can be assumed that the kurgan's soil began to develop at least between this interval. The soil development continued after construction, thus this interval can only be considered as the maximum age of the soil. The kurgan is younger than the shell (5175 $\pm$ 129 cal BP yr) simply because the shell was found in the kurgan (between the depth of 360–370 cm). However, these calibrated ages do not provide exact indications when dating the mound because of the high reservoir effect of the soil and the reservoir effect of the mollusk (*Unio* shell). This reservoir effect leads to a high uncertainty of the radiocarbon data [42,75]. The residence time of organic matter in the soils is high, and a 1–2 kyrs difference can be noticed between the calibrated age of soils and the calibrated age of shells. Considering these facts, the kurgan may be Yamnaya but it may also be younger. Taking into account the preliminary archaeological study of the kurgan (see Introduction), the fact that most of the burial mounds in the lowland region of the Carpathian Basin are of

Yamnaya culture, with the characteristic appearance of multiple levels of construction [9], we can hypothesize that it was built by the people of the Yamnaya culture, based on the radiocarbon ages, although the exact date of the construction of the kurgan cannot be determined. This could be made even more certain by a further radiocarbon analysis of the kurgan, or by locating the possible burial site, which is difficult to do because of the ex-lege protection of the kurgan.

The study of the snail fauna clearly indicates the presence of a dry ecological island after the formation of the kurgan body, with open vegetation and the development of Chernozem soil. It should be noted that the elements considered as forest-steppe species in the lowland environment are not exclusively inhabitants of that forest and forest-steppe environment described by botanists, but are in fact shade-loving elements based on the measurements of ecological tolerance of some terrestrial snail species under laboratory conditions [76]. In other words, forest-steppe species such as *Vallonia costata, Cepaea vindobonensis, Helix pomatia* also can be found in tall grass steppes where stable shading of the surface exists. Thus, their environment can be described as steppe instead of forest-steppe with scattered trees. Thus, the steppe environment in the kurgan and its close surroundings can be supported by the malacological analysis.

The possibility of extending the data about the vegetation to the wider surroundings of the kurgan is also questionable. On the locally spatial scale, the area of the kurgan forms a dry island of steppe vegetation, based on the summary of our malacological and pollen data. On the other hand, based on the literature, in a wider environment of 10–100 km^2, a general forest-steppe could have developed as a result of the mosaics of watercourses, gallery forests along the Tisza floodplain and open steppe [35,70]. This double (local—macro-regional) environmental (vegetation) mosaicism of the lowland is fundamental for understanding the vegetation and vegetation development of the Hungarian Great Plain because different vegetation associations could have developed side by side. The geoarchaeological study of the Császárné Mound shows how a small part of these mosaics can be formed by human activity (modified topography) and how these activities can modify areas even on the smallest scale.

6. Conclusions

The Császárné Mound is located in the Danube-Tisza Interfluve region of the Hungarian Great Plain. The investigation of the mound facilitated the reconstruction of the former local environment before and during the construction of the kurgan and its effect on the local environment. The analysis of the kurgan—which is based on macroscopic analyses, loss on ignition, magnetic susceptibility (MS), grain size composition examinations of the samples from a drilling section of 4.9 m—suggest three different construction phases. Based on our data, the upper layers of the original meadow Chernozem soil were used for the construction, which developed the loessy sediment that accumulated on former river bank sediments.

The radiocarbon results, despite the high uncertainty as to the actual age of the kurgan, do not exclude the hypothesis of previous archaeological investigations on other kurgans from the Hungarian Great Plain, that the kurgan may have been built by people of the Late Copper and Early Bronze Age Yamnaya culture, similarly to many burial mounds in the area. However, no grave(s) were detected when drilling (or mapping and sampling).

The reconstruction of the former environment of the kurgan suggests that steppe vegetation, mainly grasses, very similar to the present one, was present in the immediate vicinity of the kurgan's area. In addition, the construction of the kurgan created a prominent anthropogenic geomorphological form that also functioned as a dry biogeographical island, whereby the former water-affected meadow Chernozem soil was transformed into a classical Chernozem soil due to the lack of groundwater influence, which affected the original surface soil. These results are clearly indicated by the grass-dominant steppe elements in the pollen composition and also in the change of the terrestrial snail species. In this way, this kurgan is a good example of how small-scale human impacts—in the

time of prehistoric cultures—could modify environments and microhabitats, detectable even thousands of years later by complex geoarchaeological investigations of the soils and sediments of these prominent archaeological monuments.

Author Contributions: Conceptualization, P.C., D.M., P.S.; methodology, P.C., D.M., P.S.; software, P.C.; validation, P.C., D.M. and P.S.; formal analysis, P.C.; investigation, P.C., D.M., L.M.; resources, P.S.; data curation, P.C.; writing—original draft preparation, P.C.; writing—review and editing, P.C., D.M., P.S.; visualization, P.C.; supervision, D.M., P.S.; project administration, P.C., P.S.; funding acquisition, P.S. All authors have read and agreed to the published version of the manuscript.

Funding: This research was supported by the Hungarian Human Resource Development Operational Program under project code: EFOP-3.6.1-16-2016-00008 'ICER' and Ministry of Human Capacities, Hungary grant 20391-3/2018/FEKUSTRAT.

Data Availability Statement: The data presented in this study are available on request from the corresponding author. The data are not publicly available due to the data will also be used in ongoing research.

Conflicts of Interest: The authors declare no conflict of interest.

References

1. Sümegi, P.; Bede, Á.; Szilágyi, G. Régészeti geológia, geoarcheológiai és környezettörténeti elemzések régészeti lelőhelyeken. A földtudományok és a régészet kapcsolata. Analyses of Archeological Geology, Geoarcheology and Environmental History on the Archeological Sites Contat between Earth Sciences and Archeology. *Archeometriai Műhely* **2015**, *12*, 135–150.
2. Fidan, E. Geo-archaeological and geophysical investigation on the Early Bronze age layers of Tavşanli Höyük (Inland Western Anatolia). *Mediterr. Archaeol. Archaeom.* **2021**, *21*, 211–225.
3. Sapir, Y.; Sarah, P.; Sapir, Y.; Katz, H.; Faust, A. Topsoil formation processes as indicated from geoarchaeological investigations at Tel 'eton, Israel, and its environment. *Mediterr. Archaeol. Archaeom.* **2021**, *21*, 85–110.
4. Liritzis, I.; Drivaliari, A.; Vafiadou, A. A review of archaeometric results on Sarakenos Cave, Greece: First stable isotope data (^{18}O and ^{13}C) on mullusk shell (*Unio* sp.) including OSL dating and characterization-provenance of ceramics by PXRF. *Sci. Cult.* **2021**, *7*, 93–110.
5. Liritzis, I.; Oikonomou, A. An updated overview of archaeological sciences research in insular Greek Aegean Islands. *Mediterr. Archaeol. Archaeom.* **2021**, *21*, 1–27.
6. Derese, C.; Vandenberghe, D.A.G.; van Gils, M.; Vanmontfort, B.; Meirsman, E.; Mees, F.; van den Haute, P. Establishing a chronology for landscape evolution around a final palaeolithic site at Arendonk-Korhaan (NE Belgium): First results from optically stimulated luminescence dating. *Mediterr. Archaeol. Archaeom.* **2010**, *10*, 43–51.
7. Kinnaird, T.C.; Dixon, J.E.; Robertson, A.H.F.; Peltenburg, E.; Sanderson, D.C.W. Insight on topography development in the Vasilikós and Dhiarizos Valleys, Cyprus, from integrated OSL and landscape studies. *Mediterr. Archaeol. Archaeom.* **2013**, *13*, 49–62.
8. Zhen, Q. Exploring the Early Anthropocene: Implications from the long-term human-climate ineractions in Early China. *Mediterr. Archaeol. Archaeom.* **2021**, *21*, 133–148.
9. Dani, J.; Horváth, T. *Őskori Kurgánok a Magyar Alföldön. A Gödörsíros (Jamnaja) Entitás Magyarországi Kutatása az Elmúlt 30 Év során. Áttekintés és Revízió*; Archaeolingua Alapítvány: Budapest, Hungary, 2012; p. 215.
10. Rouard, X. Did indo-european languages stem from a trans-eurasian original language? An interdisciplinary approach. *Sci. Cult.* **2022**, *8*, 15–49.
11. Ecsedy, I. *The People of the Pit-Grave Kurgans in Eastern Hungary*; Fontes Archaeologici Hungaricae; Akadémiai Kiadó: Budapest, Hungary, 1979; p. 147.
12. Horváth, T.; Dani, J.; Pető, Á.; Pospieszny, L.; Svingor, É. Multidisciplinary Contributions to the Study of Pit Grave Culture Kurgans of the Great Hungarian Plain. In *Transition to the Bronze Age—Interregional Interaction and Socio-Cultural Change in the Third Millennium BC Carpathian Basin and Neighbouring Regions*; Heyd, V., Kulcsár, G., Szeverényi, V., Eds.; Conference Paper The 16th EAA Annual Meeting in Hague; Archeolingua: Budapest, Hungary, 2010; pp. 153–181.
13. Demkin, V.A.; Kashirskaya, N.N.; Demkina, T.S.; Khomutova, T.E.; El'tsov, M.V. Paleosol studies of burial mounds in the Ilovlya River valley (the Privolzhskaya Upland). *Eurasian Soil Sci.* **2008**, *41*, 115–127. [CrossRef]
14. Rowinska, A.; Sudnik-Wójcikowska, B.; Moysiyenko, I.I. Kurgans–Cultural heritage in the anthropogenic landscape of the steppe and forest steppe zones through the eyes of an archaeologist and botanist. *Wiad. Bot.* **2010**, *54*, 7–20.
15. Deák, B.; Tóthmérész, B.; Valkó, O.; Sudnik-Wójcikowska, B.; Moysiyenko, I.I.; Bragina, T.M.; Apostolova, I.; Dembicz, I.; Bykov, N.I.; Török, P. Cultural monuments and nature conservation: A review of the role of kurgans in the conservation and restoration of steppe vegetation. *Biodivers. Conserv.* **2016**, *25*, 2473–2490. [CrossRef]
16. Ionesov, V.I. Cenotaphs in ritual practice of complex societies: Proto-Bactrian cultural context. *Mediterr. Archaeol. Archaeom.* **2020**, *20*, 91–105.
17. Kaiser, E.; Winger, K. Pit graves in Bulgaria and the Yamnaya Culture. *Praehist. Z.* **2015**, *90*, 114–140. [CrossRef]

18. Bede, Á.; Salisbury, R.B.; Csathó, A.I.; Czukor, P.; Páll, D.P.; Szilágyi, G.; Sümegi, P. Report of the complex geoarcheological survey at the Ecse-halom kurgan in Hortobágy, Hungary. *Cent. Eur. Geol.* **2015**, *58*, 268–289. [CrossRef]
19. Pál, B.A.S.; Katalin, J. Joó Adatok a Hortobágy paleoökológiai rekonstrukciójához a Csípő-halom talajtani és malakológiai vizsgálata alapján. *Földtani Közlöny* **2003**, *133*, 421–432.
20. Barczi, A. The importance of pedological investigations in Holocene palaeoecological reconstructions. *Antaeus* **2004**, *27*, 129–134.
21. Joó, K.; Barczi, A.; Sümegi, P. Study of soil scientific, layer scientific and palaeoecological relations of the Csípő-mound kurgan. *Atti Soc. Toscana Sci. Nat.* **2007**, *A112*, 141–144.
22. Borisov, A.V.; Krivosheev, M.; Mimokhod, R.A.; El'tsov, M. "Sod blocks" in kurgan mounds: Historical and soil features of the technique of tumuli erection. *J. Archaeol. Sci.* **2019**, *24*, 122–131. [CrossRef]
23. Rómer, F. *Compte-Rendu de la Huitième Session à Budepest 1876. I. Résultats Généreaux du Mouvement Archéologique en Hongrie*; Magyar Nemzeti Múzeum: Budapest, Hungary, 1878; p. 187.
24. Alexandrovskiy, A.L. Natural Environment as Seen in Soil. *Eurasian Soil Sci.* **1996**, *29*, 245–254.
25. Mitusov, A.V.; Mitusova, O.E.; Pustovoytov, K.; Lubos, C.C.-M.; Dreibrodt, S.; Bork, H.-R. Palaeoclimatic indicators in soils buried under archaeological monuments in the Eurasian steppe: A review. *Holocene* **2009**, *19*, 1153–1160. [CrossRef]
26. Zaitseva, G.I.; Chugunov, K.V.; Bokovenko, N.A.; Dergachev, V.I.; Dirksen, V.G. Chronological study of archaeological sites and environmental change around 2600 BP in the Eurasian steppe belt (Uyuk Valley, Tuva Republic). *Geochronometria* **2005**, *24*, 97–107.
27. Alexandrovskiy, A.L. Holocene Development of Soils in Response to Environmental Changes: The Novosvobodnaya Archaeological Site, North Caucasus. *Catena* **2000**, *41*, 238–248. [CrossRef]
28. Demkin, V.A.; Klepikov, V.M.; Udaltsov, S.; Demkina, T.; Eltsov, M.V.; Khomutova, T. New aspects of natural science studies of archaeological burial monuments (kurgans) in the southern Russian steppes. *J. Archaeol. Sci.* **2014**, *42*, 241–249. [CrossRef]
29. Sümegi, P. *A Negyedidőszak Földtanának és Őskörnyezettanának Alapjai*; JATE Press: Szeged, Hungary, 2002; 262p.
30. Persaits, G.; Sümegi, P. Régészeti lelőhelyekről származó fitolit vizsgálatok jelentősége az archeobotanikában. In *Komplex Archeobotanika*; Törocsik, T., Náfrádi, K., Sümegi, P., Eds.; GeoLitera: Szeged, Hungary, 2015; pp. 145–154.
31. Szilágyi, G.; Sümegi, P.; Molnár, D.; Sávai, S. Mollusc-based paleoecological investigations of the Late Copper—Early Bronze Age earth mounds (kurgans) on the Great Hungarian Plain. *Cent. Eur. J. Geosci.* **2015**, *5*, 465–479. [CrossRef]
32. Hungarian National Museum Archaeological Database. Available online: https://archeodatabase.hnm.hu/hu/node/42649 (accessed on 15 December 2021).
33. Molnár, B. *A Kiskunsági Nemzeti Park Földtana és Vízföldtana*; JATE Press: Szeged, Hungary, 2015; p. 524.
34. Stefanovits, P. *Talajtan*; Mezőgazda Kiadó: Budapest, Hungary, 1972; p. 380.
35. Sümegi, P.; Persaits, G.; Gulyás, S. *Woodland-Grassland Ecotonal Shifts in Environmental Mosaics: Lessons Learnt from the Environmental History of the Carpathian Basin (Central Europe) during the Holocene and the Last Ice Age Based on Investigation of Paleobotanical and Mollusk Remains*; Springer Press: New York, NY, USA, 2012; pp. 17–57.
36. Holdridge, L.R. Determination of world plant formations from simple climatic data. *Science* **1947**, *105*, 367–368. [CrossRef]
37. Péczely, G. *Éghajlattan*; Nemzeti Tankönyvkiadó: Budapest, Hungary, 1979; p. 342.
38. Wikimedia Commons. Pannonian Basin Geographic Map Blank Cropped. Available online: https://upload.wikimedia.org/wikipedia/commons/2/27/Pannonian_Basin_geographic_map_blank_croped.svg (accessed on 17 December 2021).
39. Gyalog, L.; Síkhegyi, F. *Magyarország Földtani Térképe, M=1:100,000*; A Magyar Állami Földtani Intézet Kiadványa: Budapest, Hungary, 2005.
40. Arcanum. Military Survey of Hungary. 1941. Available online: https://maps.arcanum.com/hu/map/hungary1941/?layers=29&bbox=2048733.8922147613%2C5974534.368118141%2C2339653.221868142%2C6082463.45205681 (accessed on 17 December 2021). (In Hungarian).
41. Google Maps. Available online: https://goo.gl/maps/n5twBG8njBKdCgSR9 (accessed on 17 December 2021).
42. Birks, H.J.B.; Birks, H.H. *Quaternary Paleoecology*; Edward Arnold Press: London, UK, 1980; p. 289.
43. Munsell, A.H. *Munsell Soil Color Charts*; Munsell Color Company: Baltimore, MD, USA, 2000; p. 29.
44. IUSS Working Group WRB. *World Reference Base for Soil Resources 2014, Update 2015. International Soil Classification System for Naming Soils and Creating Legends for Soil Maps*; World Soil Resources Reports No. 106; FAO: Rome, Italy, 2015.
45. Michéli, E.; Csorba, A.; Szegi, T.; Dobos, E.; Fuchs, M. The soil types of the modernized, diagnostic based Hungarian Soil Classification System and their correlation with the World reference base for soil resources. *Hung. Geogr. Bull.* **2019**, *68*, 109–117. [CrossRef]
46. Bokhorst, M.P.; Vandenberghe, J.; Sümegi, P.; Łanczont, M.; Gerasimenko, N.P.; Matviishina, Z.N.; Markovic, S.B.; Frechen, M. Atmospheric circulation patterns in central and eastern Europe during Weichselian Pleniglacial inferred from loess grain-size records. *Quat. Int.* **2011**, *234*, 62–74. [CrossRef]
47. Sümegi, P.; Molnár, D.; Gulyás, S.; Náfrádi, K.; Sümegi, B.P.; Törőcsik, T.; Persaits, G.; Molnár, M.; Vandenberghe, J.; Zhou, L. High-resolution proxy record of the environmental response to climatic variations during transition MIS3/MIS2 and MIS2 in Central Europe: The loess-paleosol sequence of Katymár brickyard (Hungary). *Quat. Int.* **2019**, *504*, 40–55. [CrossRef]
48. Wentworth, C.K. A Scale of grade and class terms for clastic sediments. *J. Geol.* **1922**, *30*, 377–392. [CrossRef]
49. Dearing, J. *Environmental Magnetic Susceptibility: Using the Bartington MS2 System*; Chi Publishing: Keniloworth, UK, 1999; p. 43.
50. Dean, W.E. Determination of carbonate and organic matter in calcareous sediments and sedimentary rocks by loss on ignition; comparison with other methods. *J. Sediment. Petrol.* **1974**, *44*, 242–248.

51. Hieri, O.; Lotter, A.; Lemcke, G. Loss on Ignition as a Method for Estimating Organic and Carbonate Content in Sediments: Reproducibility and Comparability of Results. *J. Paleolimnol.* **2001**, *25*, 101–110. [CrossRef]
52. Hertelendi, E.; Csongor, É.; Záborszky, L.; Molnár, I.; Gál, I.; Győrffy, M.; Nagy, S. Counting system for high precision C-14 dating. *Radiocarbon* **1989**, *32*, 399–408. [CrossRef]
53. Molnár, M.; Janovics, R.; Major, I.; Orsovszki, J.; Gönczi, R.; Veres, M.; Leonard, A.G.; Castle, S.M.; Lange, T.E.; Wacker, L. Status report of the new AMS 14C sample preparation lab of the Hertelendi Laboratory of Environmental Studies (Debrecen, Hungary). *Radiocarbon* **2013**, *55*, 665–676. [CrossRef]
54. Demény, A.; Schöll-Barna, G.; Fórizs, I.; Osán, J.; Sümegi, P.; Bajnóczi, B. Stable isotope compositions and trace element concentrations in freshwater bivalve shells (*Unio* sp.) as indicators of environmental changes at Tiszapüspöki, eastern Hungary. *Cent. Eur. Geol.* **2012**, *55*, 441–460. [CrossRef]
55. Gulyás, S.; Sümegi, P.; Molnár, M. New radiocarbon dates from the Late Neolithic tell settlement of Hódmezővásárhely-Gorzsa, SE Hungary. *Radiocarbon* **2010**, *52*, 1458–1464. [CrossRef]
56. Hertelendi, E.; Sümegi, P.; Szöör, G. Geochronologic and paleoclimatic characterization of Quaternary sediments in the Great Hungarian Plain. *Radiocarbon* **1992**, *34*, 833–839. [CrossRef]
57. Schöll-Barna, G. Kagyló- és csigahéjak stabilizotóp-vizsgálata: Környezet- és klíma-rekonstrukció a Balaton vízgyűjtőjében. Szegedi Tudományegyetem, Környezettudományi Doktori Iskola. Ph.D. Thesis, University of Szeged: Szeged, Hungary, 2011; p. 114.
58. Reimer, P.; Austin, W.; Bard, E.; Bayliss, A.; Blackwell, P.G.; Ramsey, C.B.; Butzin, M.; Cheng, H.; Edwards, R.L.; Friedrich, M. The IntCal20 Northern Hemisphere radiocarbon age calibration curve (0–55 cal kBP). *Radiocarbon* **2020**, *62*, 725–757. [CrossRef]
59. Philippsen, B. The freshwater reservoir effect in radiocarbon dating. *Herit. Sci.* **2013**, *1*, 24. [CrossRef]
60. Krolopp, E. A Buda Környéki Alsópleisztocén Mésziszapok Csiga-Faunájának Állatföldrajzi Ökológiai Vizsgálata. Ph.D. Thesis, Eötvös Loránd University: Budapest, Hungary, 1958; p. 141.
61. Magyari, E.; Sümegi, P.; Braun, M.; Jakab, G. Retarded hydrosere: Anthropogenic and climatic signals in a Holocene raised bog profile from the NE Carpathian Basin. *J. Ecol.* **2001**, *89*, 1019–1032. [CrossRef]
62. Moore, P.D.; Webb, J.A.; Collinson, M.E. *Pollen Analysis*; Blackwell Scientific Publications: Oxford, UK, 1991.
63. Reille, M. *Pollen et Spores d'Europe et d'Afrique du Nord*; Laboratoirede Botanique Historique et Palynologie: Marseille, France, 1992.
64. Maher, L.J. Nomograms for computing 0.95 confidence limits of pollen data. *Rev. Palaeobot. Palynol.* **1972**, *13*, 85–93. [CrossRef]
65. Sümegi, P.; Magyari, E.; Dániel, P.; Hertelendi, E.; Rudner, E. A kardoskúti Fehér-tó negyedidőszaki fejlődéstörténetének rekonstrukciója. *Földtani Közlöny* **1999**, *129*, 479–519.
66. Allen, J.R.M.; Watts, W.A.; Huntley, B. Weichselian palynostratigraphy, palaeovegetation and palaeoenvironment: The record from Lago Grande di Monticchio, southern Italy. *Quat. Int.* **2000**, *73–74*, 91–110. [CrossRef]
67. Behre, K.E. The interpretation of anthropogenic indicators in pollen diagrams. *Pollen Spores* **1981**, *23*, 225–245.
68. Behre, K.E. (Ed.) *Anthropogenic Indicators in Pollen Diagrams*; Balkema Press: Boston, MA, USA, 1986; p. 232.
69. Elenga, H.; Peyron, O.; Bonnefille, R.; Jolly, D.; Cheddadi, R.; Guiot, J.; Hamilton, A.C. Pollen-based biome reconstruction for southern Europe and Africa 18,000 yr bp. *J. Biogeogr.* **2000**, *27*, 621–634. [CrossRef]
70. Magyari, E.K.; Chapman, J.C.; Passmore, D.G.; Allen JR, M.; Huntley, J.P.; Huntley, B. Holocene persistence of wooded steppe in the Great Hungarian Plain. *J. Biogeogr.* **2010**, *37*, 915–935. [CrossRef]
71. Prentice, I.C.; Guiot, J.; Huntley, B.; Jolly, D.; Cheddadi, D. Reconstructing biomes from palaeoecological data: A general method and its application to European pollen data at 0 and 6 ka. *Clim. Dyn.* **1996**, *12*, 185–194. [CrossRef]
72. Prentice, I.C.; Webb, T. BIOME 6000: Reconstructing global mid-Holocene vegetation patterns from palaeoecological records. *J. Biogeogr.* **1998**, *25*, 997–1005. [CrossRef]
73. Tarasov, P.; Webb, T.; Andreev, A.A.; Afanas'eva, N.B.; Berezina, N.A.; Bezusko, L.G.; Blyakharchuk, T.A.; Bolikhovskaya, N.S.; Cheddadi, R.; Chernavskaya, M.M.; et al. Present-day and mid-Holocene biomes reconstructed from pollen and plant macrofossil data from the former Soviet Union and Mongolia. *J. Biogeogr.* **2002**, *25*, 1029–1053. [CrossRef]
74. Gerling, C.; Bánffy, E.; Dani, J.; Kohler, K. Immigration and transhumance in the Early Bronze Age Carpathian Basin: The occupants of a kurgan. *Antiquity* **2012**, *86*, 1097–1111. [CrossRef]
75. Zhou, W.; Head, M.J.; Wang, F.; Donahue, D.J.; Jull, A.J.T. The reliability of AMS radiocarbon dating of shells from China. *Radiocarbon* **1999**, *41*, 17–24. [CrossRef]
76. Ant, T.H. Faunistische, ökologische und tiergeographische Untersuchungen zur Verbreitung der Landschnecken in Nordwestdeutschland. *Abh. Landesmus. Nat. Münster* **1963**, *25*, 125.